Recoil-ion–projectile-ion–cusp-electron triple-coincidence measurements for 1-MeV/u bare and one-electron O and C projectiles on Ne

J. Freyou, M. Breinig, C. C. Gaither III, and T. A. Underwood
Department of Physics, University of Tennessee, Knoxville, Tennessee 37996-1200
and Oak Ridge National Laboratory, Oak Ridge, Tennessee 37831-6377
(Received 23 June 1989; revised manuscript received 28 August 1989)

We have measured in coincidence the projectile-ion charge state, the target-recoil-ion charge state, and the energy of a free electron (cusp electron) emerging from the same collision with a velocity close to the beam velocity, for 1-MeV/u bare and one-electron oxygen and carbon projectiles colliding with neon targets. The most probable recoil-ion charge state of recoil ions not associated with cusp electrons is 1. Most cusp electrons accompany a projectile that does not change charge, and the most probable recoil-ion charge state in this case lies between 2 and 3. The recoil-ion charge-state distribution associated with a cusp electron and bound-state capture by the projectile is shifted towards even higher charge states. Cusp-electron production in conjunction with electron loss by the projectile is not associated with such a large shift. The probability of cusp-electron production given the production of a recoil ion increases with increasing recoil-ion charge state for projectiles that do not change charge and for projectiles that capture an electron, and decreases with increasing recoil-ion charge state for projectiles that lose an electron in the collision.

I. INRODUCTION

Fast collisions between highly charged heavy ions and neutral gas targets are characterized by many processes such as projectile and target excitation and ionization and target electron transfer to projectile-centered bound and continuum states.

Large-impact-parameter collisions between MeV/u highly charged projectile ions and neutral target atoms can eject many electrons from a single target atom and have been shown to excite the inner atomic shells of the target.[1] Energy transferred to the target atom in the form of excitation and ionization energy is, on the average, many times greater than energy transferred to it as kinetic energy. The kinetic energy of target recoil ions is low. For a neon target it does not exceed 10 eV until K-shell electrons are removed from the target atom.[2] Slow recoil ions created by fast projectile ions were first studied by Cocke[3] in the late 1970s.

Recent measurements of scattering angle, recoil-ion charge state, and inelasticity in MeV/u collisions find that the projectile inelastic energy loss for multiple target ionization far exceeds the sum of the ionization potentials of the target.[4,5] Recoil-ion energy, target-atom excitation, and, in the case of charge transfer, balance between energy gain due to an increase in binding energy on the projectile and energy loss due to the captured electron's translational energy cannot account for this difference. A large fraction of the total energy lost by the projectile is carried off by continuum electrons.

A cusp-shaped peak is observed in the velocity distribution of electrons emitted in fast ion-atom collisions. This peak is centered at the projectile-ion velocity, where the continuum electron's velocity matches the beam velocity in both speed and direction. Continuum electrons emitted in ion-atom collisions with a velocity close to the beam velocity are commonly called cusp electrons. Do cusp electrons significantly contribute to the inelasticity of the collision? Two primary processes produce the cusp-electron peak, projectile-electron loss to the continuum (ELC), and target-electron capture to the continuum (ECC). ELC is a low-momentum-transfer process involving an electron, in a bound state of the projectile, being excited to a continuum state of the projectile. ECC is a high-momentum-transfer process involving an electron, in a bound state of the target atom, being captured to a projectile-centered continuum state. The relative importance of these two processes in producing an observed cusp is strongly dependent on the projectile-ion charge state and on the projectile velocity. For bare projectiles ECC is the only possible process, whereas for one- or two-electron projectiles the two processes can become almost equally probable.[6]

In our experiment 1-MeV/u bare and one-electron carbon and oxygen projectiles collide with neon target atoms at pressures of 1–8 mTorr. We simultaneously measure the projectile-ion exit charge state and the target-recoil-ion charge state and determine whether or not a cusp electron has been produced. We determine if collisions in which a cusp electron is produced are characterized by different recoil-ion–projectile-ion charge-state distributions and if cusp-electron production significantly influences the inelasticity in collisions involving multiple target ionization. Related experiments, investigating the dependence of the shape of the energy spectrum of δ electrons on the charge states of the projectile and the recoil ion for 0.53 MeV/u $F^{8,9+}$ projectiles on Ne have been carried out by other investigators.[7]

II. THEORETICAL APPROACHES

Multiple ionization of rare-gas atoms by fast projectile ions within a single collision is a true quantum-

mechanical many-body problem with particle emission under nonperturbative conditions. If the relative velocity of the projectile is close to the orbital velocity of the electrons being detached, perturbative methods are generally invalid,[2] and solving the many-electron, time-dependent Schrödinger equation is beyond the scope of present-day computational facilities for such a scattering problem. Calculations of ionization cross sections are therefore carried out within the framework of the independent-electron approximation (IEA).

McGuire and Weaver[8] have presented a semiclassical derivation of the IEA for atomic scattering by heavy particles and the consequent binomial distribution of single-electron probabilities. Here they have shown that multiple-ionization transition probabilities can be obtained from transition probabilities calculated in a one-electron formalism. Within the framework of the time-dependent Hartree-Fock approximation (TDHF) one might calculate these single-electron cross sections. However, the solution of the TDHF problem for multiple ionization in multiply ionizing collisions encounters difficulties even for a two-electron atom, and further approximations are necessary.

One method of calculating the single-electron transition probabilities is the three-body, three-dimensional classical trajectory Monte Carlo (CTMC) method developed by Olson.[9] This method includes all forces between the incident ion, the active electron, and the target nucleus. The CTMC method, however, is only directly applicable to hydrogenic target atoms. To calculate transition probabilities in multielectron atoms, it is necessary to extend the representation of the target electron so that it profiles the electron shell under consideration. The CTMC method has been successfully used to predict total as well as partial ionization cross sections for various collision systems.

The newly developed n-body classical-trajectory Monte Carlo (nCTMC) method explicitly incorporates all electrons in the collision.[10] It includes all forces between the projectile ion and the target nucleus and its electrons and all forces between the target nucleus and its electrons. Excluded are the electron-electron interactions which are approximated by using effective charges between the electrons and their parent nucleus. The nCTMC method allows for the first time the determination of the angular distributions and energies of the recoil ions, the projectile ions, and the ejected electrons. For 1.14-MeV/u $U^{32+}+Ne$ collisions nCTMC cross sections, differential in scattering angle of projectile ion, recoil ion, and ejected electron, have been presented as a function of the recoil-ion charge state.[11] For 10-MeV $C^{5,6+}$ ions on Ne cross sections for the production of Ne^{+} and Ne^{4+} recoil ions as a function of the projectile scattering angle, and the projectile inelastic energy loss as a function of the degree of target ionization, calculated by the nCTMC method, have been published.[4] Calculations have been successfully compared with experimental results.[4,10,11]

III. EXPERIMENTAL APPARATUS

Fast projectile ions from the Oak Ridge National Laboratory EN Tandem Van de Graaff accelerator pass through a 90° analyzing magnet and ions of a selected momentum to charge ratio (p/q) are then carbon-foil stripped to higher charge states. A switching magnet then passes only bare or hydrogenic projectile ions. The pressure in the beamline leading to the experimental chamber remains below 10^{-6} Torr to minimize charge exchange in collisions with background gas so that the ion charge state entering the experiment is pure.

Two sets of four jaw slits, placed several meters apart, collimate the beam to less than a 1-mm^2 area and a 1-mrad angular divergence on target. The target gas cell, the recoil-ion spectrometer, and the cusp-electron spectometer are located in the experimental chamber (see Fig. 1) which is lined with two layers of μ-metal magnetic shielding. The chamber is maintained at a pressure of less than 10^{-5} Torr when millitorr pressures exist in the

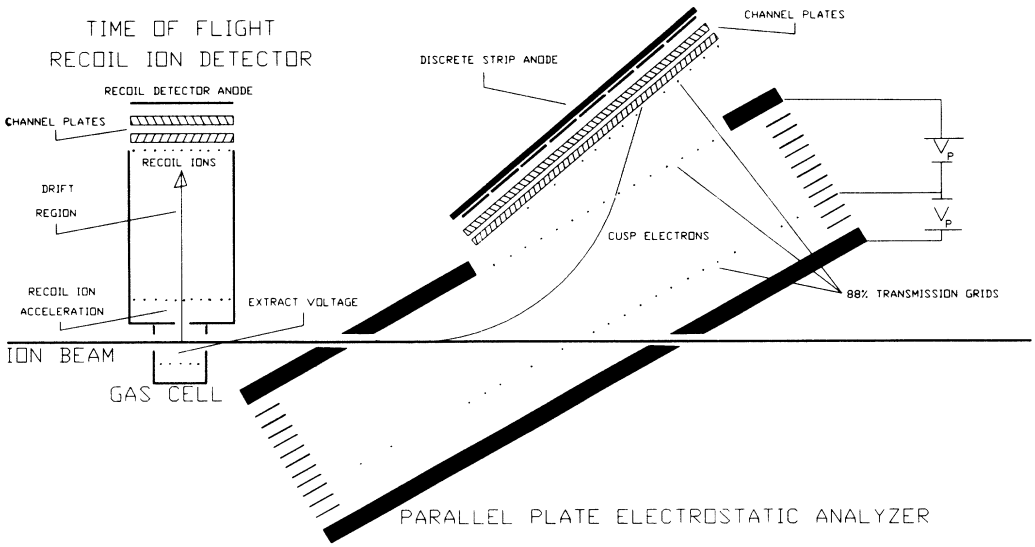

FIG. 1. Experimental apparatus.

gas cell. Recoil ions are extracted by a very weak electric field ($\sim$7 V/cm) into the time-of-flight (TOF) recoil-ion spectrometer. Cusp electrons are deflected and energy is analyzed in the parallel-plate spectrometer. The electric field in this spectrometer ($\sim$50 V/cm) does not appreciably deflect the projectile ions which exit through a hole in the back of the spectrometer. The electric field of the electrostatic charge-state analyzer separates the projectile-ion charge states for detection by a discrete dynode electron multiplier. The target-gas-cell region, an integral part of the TOF recoil-ion spectrometer, is only 1 cm long. The pressure in the target gas cell is measured by a Baratron differential capacitive manometer. The pressure at the Baratron head is proportional to but not necessarily equal to the pressure in the interaction region due to the apertures near the interaction region which allow the beam to pass through the gas cell and the recoil ions to escape perpendicular to the beam direction. The beam entry and exit apertures are 2.4 mm in diameter and the recoil-ion aperture is 3.2 mm in diameter. The gas cell has a volume of about 4 cm^3 and the beam passes 3 mm below the recoil-ion aperture. A grid 1 cm below the beam path allows us to place a small recoil-ion extraction voltage across the cell. The electric field in the gas cell due to this extraction voltage must be sufficiently small to allow the cusp electrons which move with the beam velocity ($\sim$545 eV) to escape without being noticeably deflected.

A simple TOF spectrometer consists of a region of constant electric field, which contains the source of the charged particles, followed by a field-free drift region terminating with a particle detector. If all ions were formed with zero initial velocity at a point source or in a plane whose normal is parallel to the electric field in the gas cell, all ions with the same q/m would have the same flight time to the detector. In practice, however, one has a source with a finite width along the field direction. A spread in the flight times of ions with the same q/m is therefore introduced due to path length differences. An additional time spread is introduced by the initial kinetic energy distribution of the ions at the source. Wiley and McLaren[12] showed that a reduction in time spread due to the initial space distribution, called space focusing, can be realized if a second accelerating region is placed just after the first. If the lengths of the two accelerating regions and the drift region and the ratio of the electric fields in the two accelerating regions are chosen properly, charged particles with the same q/m created at different depths in the first region have the same flight time to the detector. In our experiment the conditions for space focusing are satisfied and space focusing is experimentally verified by varying the voltage across the second accelerating region about the calculated value and observing an increase in time spread. The time spread due to the initial kinetic energy of the recoil ions, however, cannot be reduced in our experiment. A reduction here requires increasing the ratio of an ion's total kinetic energy to its initial kinetic energy at the source. We must, however, minimize the strength of the field in the first accelerating region, since too large a field not only extracts low-energy recoil ions from the beam-gas interaction region but also changes the trajectories of cusp electrons sufficiently to prevent them from exiting the gas cell into the electron spectrometer. We therefore are only able to resolve, by their different flight times to the detector, charge states 1–5 of neon recoil ions produced in our experiments. Figure 2 shows a recoil-ion TOF spectrum for C^{6+} projectiles on Ne (6 mTorr) measured in coincidence with one bound-state capture. Ne isotopes are not resolved.

Cusp electrons emerge from the interaction region nearly undeflected and enter a large 30° parallel-plate electrostatic analyzer. The interaction region (the center of the gas cell) coincides with the entrance focus of the analyzer. In the analyzer the electron trajectories are bent into a large detector located in the exit focal plane of the analyzer. A 30° analyzer has second-order focusing in the plane of deflection.[13] Thus electrons with the same energy leaving the entrance focus with trajectories whose projections onto the plane of deflection make an angle $\theta = 30° \pm \Delta\theta$ with the ground plate are focused onto a line in the focal plane. Electrons with different energies are focused onto different parallel lines. Their position along these focal lines is determined by their emission angle perpendicular to the plane of deflection. If the acceptance angle in the plane of deflection is limited to a narrow range of angles about 30°, and a wide range of angles is accepted perpendicular to the plane of deflection, then the energy and angular distribution of electrons emitted in a plane perpendicular to the plane of deflection will be imaged in the focal plane. For our analyzer, the half-angle of acceptance in the plane of deflection is 5° and the half-angle of acceptance perpendicular to the plane of deflection is 10°. The ratio of the maximum to the minimum energy of electrons which can be detected is 1.42. A channel plate mounted in the focal plane of the 30° analyzer, followed by a copper collector, serves as our cusp-electron detector. The collector is designed to allow us to measure the energy and angular distribution of cusp electrons. The anode is made of discrete strips which consist of insulating material with a copper coating on one side. The insulating sides of the strips are inserted into shallow recesses of a large slab of copper which is connected to ground via a capacitor. This design effectively eliminates cross talk between strips, which

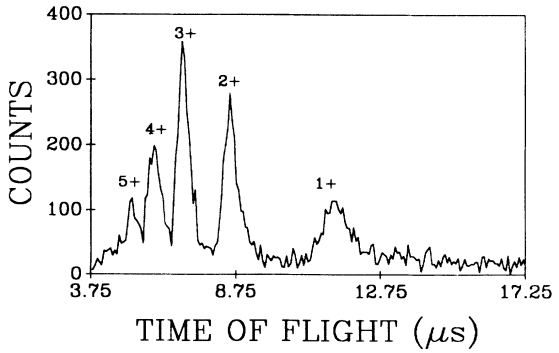

FIG. 2. Recoil-ion TOF spectrum for C^{6+} projectiles on Ne measured in coincidence with one bound-state capture.

severely plagues other anode designs. Elimination of cross talk is important when the position of the electrons' arrival in the focal plane needs to be determined. Future experiments will focus on determining this position, but the experiment described in this work is designed to measure the total cusp-electron yield. Therefore all the strips making up the anode are connected and serve as one large collector.

Working with such a large collector, background signals can become a serious problem. Early in the experiment, a large background peak was superposed onto the cusp peak. Calculations and tests of the apparatus, using an electron gun as a source of electrons, showed that this background peak resulted from cusp electrons hitting the back plate of the 30° parallel-plate spectrometer and ejecting secondary electrons. Our previous experiments with parallel-plate analyzers never used such a large open detector, capable of viewing nearly the entire volume of the spectrometer, but instead used channel-electron multipliers with apertures of less than 1 cm. Thus this background had never been observed. To eliminate the background problem, an 88% transmission grid was substituted for the back plate of the analyzer, and held at the analyzer voltage. This grid is now positioned as close to the grounded plate as possible, as to just allow the largest trajectories which can be viewed by the detector to pass below it. This then causes trajectories which intersect the grid to intersect at a point from which ejected electrons are accelerated towards the ground plate and not towards the detector. The background in the cusp peak is thus effectively eliminated.

IV. DATA ANALYSIS

The goal of this experiment is to more completely characterize collisions between 1-MeV/u bare and one-electron oxygen and carbon projectiles and neon targets by answering the following questions.

(i) If cusp electrons emerge from collisions in which neon recoil ions are produced, what is the recoil-ion charge state distribution?

(ii) If cusp electrons are produced in coincidence with a particular exit charge state of the projectile, what is the recoil-ion charge-state distribution?

(iii) If a recoil ion of a particular charge state and a projectile ion of a particular exit charge state are produced in the same collision, how probable is the production of a cusp electron?

Two sets of measurements are made. The first set of measurements is repeated at various target-gas pressures between 1 and 8 mTorr with projectiles which enter the collision with incident charge state q_{in}. In a time interval Δt we record (i) the total number of projectile ions detected leaving the collision with exit charge state q_e; (ii) the total number of recoil ions detected; (iii) the total number of cusp electrons detected; (iv) the number of recoil ions of charge state q_r detected in coincidence with a projectile ion of exit charge state q_e; and (v) the number of cusp electrons detected in coincidence with a projectile of exit charge state q_e. The second set of measurements is only made at one target-gas pressure. Measurements (i), (ii), and (iii) from above are repeated. In addition, we measure (vi) the number of recoil ions of charge state q_r detected in coincidence with a cusp electron; and (vii) the number of recoil ions of charge state q_r detected in coincidence with a cusp electron and a projectile ion of exit charge state q_e (triple coincidence).

The fraction $f_e(q_e,p)$ of projectiles exiting the gas cell with exit charge state q_e is found as a function of target-gas pressure p from the ratio of the total number of projectiles of each exit charge state q_e detected in time Δt to the total number of cusp electrons, recoil ions, or recoil-ion–cusp-electron coincidences detected in time Δt. Each charge-state fraction $f_e(q_e,p)$ is fitted to a second-order polynomial in the pressure p (in units of mTorr) for p between 1 and 8 mTorr.

$$f_e(q_e,p)=a(q_e)+b(q_e)p+c(q_e)p^2 . \tag{1}$$

The coefficient of the quadratic term $c(q_e)$ is always found to be more than three orders of magnitude smaller than the coefficient of the linear term $b(q_e)$. Each charge-state fraction is therefore a linear function of p, thus verifying single-collision conditions for projectile charge-changing collisions.

The detection efficiency of the projectile-ion detector is determined from the fraction of cusp electrons detected in coincidence with a projectile ion of any charge state. Note that each cusp electron detected is produced by a projectile ion and therefore will be detected in coincidence with a projectile ion of some exit charge state by a detector with 100% efficiency. The total number of electrons detected contains a background contribution which is found by making measurements at different target-gas pressures.

The detection efficiency of the recoil-ion spectrometer is not found for each recoil charge state separately but is averaged over all charge states. If the projectile captures an electron in an ion-atom collision, then a recoil ion is produced and will be detected by a 100% efficient detector. Similarly, if a cusp electron is produced by a bare projectile in an ion-atom collision, then a recoil ion is also produced in this collision and will be detected by a 100% efficient detector. In our measurements the recoil-ion detection efficiency averaged over all recoil-ion charge states is found to be $D_r=0.014$. The detection efficiency D_r is low because recoil ions are produced in the entire region where the ion beam interacts with the target gas, but only recoil ions produced near the recoil-ion extraction aperture are detected. Since our measurements with C^{6+} projectiles reproduce charge-state disributions measured previously with much higher extraction fields,[14,15] where negligible dependence of the recoil-ion detection efficiency on recoil-ion charge state is expected, we conclude that the recoil-ion detection efficiency does not vary appreciably with recoil-ion charge state. Charge changing by high-charge-state recoil ions in the region of the extraction field will yield asymmetric peaks. The limited resolution of our recoil-ion TOF spectrometer also results in asymmetric peaks, since Ne isotopes are not resolved. We do not observe an increase in the asymmetry of the peaks as a function of target-gas pressure between 1 and 8

mTorr. The area under the high-charge-state peaks, normalized to the total number of incident projectiles, is found to be a linear function of pressure. We therefore conclude that charge changing by high-charge-state recoil ions does not significantly influence our measured charge-state distributions.

The cusp-electron detection efficiency is estimated differently. We assume that all electrons falling into the wide energy and angular acceptance window of our spectrometer would be detected, were it not for two field-defining grids in the analyzer that must be traversed by the electrons. The transmission of the grids is calculated for the angles of electron incidence and the product of the transmissions of the two grids is used as the detection efficiency of the electron detector $D_e = 0.10$.

The probability for charge exchange under single-collision conditions is found from the coefficient $b(q_e)$ of the linear term of Eq. (1) for exit charge states $q_e = q_{\text{in}} \pm 1$. The error in $b(q_e)$ is taken to be the one standard deviation error obtained from the fit. In a separate experiment using the same apparatus the probabilities for bound-state capture and electron loss per incident ion per millitorr gas cell pressure were measured for 1-MeV/u O^{7+} projectiles on He. Using published cross sections of Hippler *et al.*,[16] the effective gas cell length l was calculated to be 1.8 cm. To calculate the charge-exchange cross sections and all other cross sections presented in this paper we use this effective gas cell length l.

The total number of cusp electrons observed per incident ion is fit to a second-order polynomial in the pressure p for p between 1 and 8 mTorr. Again the coefficient of the quadratic term is more than three orders of magnitude smaller than the coefficient of the linear term. The constant term gives the cusp-electron background while the linear term yields the cross section for the production of a cusp electron when divided by D_e and $n_0 l$. Here n_0 is the number of target atoms per cm^3 per millitorr. Again, the error in the linear term is taken to be the one standard deviation error obtained from the fit. The relative error in the cusp-electron production cross section is determined by this error in the linear term, while the absolute error also includes the error in D_e and l. We assume such systematic errors to contribute an additional $\pm 50\%$ to the uncertainty in the absolute values of the cross sections. The cusp-electron production cross section can also be calculated by summing the cross sections for the production of a cusp electron in coincidence with a projectile ion of exit charge state q_e over all exit charge states. Values obtained in this manner agree closely with those calculated from the total cusp-electron yield.

The cross section for the production of recoil ions of charge state q_r, by projectiles with exit charge state q_e, is found by assuming that the recoil-ion production probability is a second-order polynomial in the pressure p. The number of coincidences between recoil ions of charge state q_r and projectiles of exit charge state q_e per incident projectile ion is then given by

$$N(q_r,q_e) = b(q_r,q_e)p + c(q_r,q_e)p^2 \ . \tag{2}$$

$N(q_r,q_e)$ represents the observed coincidences corrected for dead time. No constant term is needed since no recoil ions are observed at zero pressure. The quadratic term is nonzero only for low-recoil-ion charge states measured in coincidence with bound-state capture or projectile-electron loss. This implies that at the higher target-gas pressures single-collision conditions for low-charge-state–recoil-ion production in coincidence with single-electron capture or loss no longer prevail and that the projectile can produce a recoil ion in one collision while it captures or loses an electron in another collision. A fit to a third-order polynomial in p was tried, but the absolute value of the coefficient of the cubic term was always more than three orders of magnitude smaller than that of the quadratic term and the coefficient was often negative. Table I gives $b(q_r,q_e)$ and $c(q_r,q_e)$ for all fits for which the coefficient of the quadratic term is no smaller than three orders of magnitude less than the coefficient of the linear term. The recoil-ion-production cross section is now found from $b(q_e,q_r)$. The error in $b(q_e,q_r)$ is taken to be the one standard deviation error obtained from the fit. Again we assume systematic errors in D_r and l to contribute an additional $\pm 50\%$ to the uncertainty in the absolute value of the cross sections. After having found the recoil-ion production cross sections and the projectile charge-changing cross sections we estimate the probability of producing a recoil ion in one collision while changing the charge state of the projectile in a second collision at 1 mTorr gas cell pressure. This probability nearly always reproduces the coefficient $c(q_r,q_e)$ of the quadratic term of Eq. (2) to within uncertainties, thus giving confidence in the values of the coefficients of the linear terms obtained from the fit.

Measurements of cusp-electron–recoil-ion coincidences and cusp-electron–recoil-ion–projectile-ion triple coincidences are only made at a single target-gas-cell pressure. The cross section for the production of a recoil

TABLE I. Coefficients of the linear and quadratic term obtained from the fit to Eq. (2).

Incident projectile	Process[a]	$b(q_r,q_e)\times 10^5$ $q_r=1+$	$q_r=2+$	$q_r=3+$	$c(q_r,q_e)\times 10^6$ $q_r=1+$	$q_r=2+$	$q_r=3+$
O^{7+}	SC	18±1	60±9		69±9	28±12	
O^{7+}	SL	0.6±0.1	0.7±0.4	1.0±0.3	1.8±0.3	1.1±0.5	0.2±0.1
C^{6+}	SC	19±3	7±3		37±10	20±12	
C^{5+}	SC	18±3	60±2	69±3	35±5	22±12	5±4
C^{5+}	SL	4.8±0.5	18±3	25±1	22±7	10±5	2±1

[a]SC represents single-electron capture and SL represents single-electron loss by the projectile.

TABLE II. Electron capture and loss cross sections for 1-MeV/u projectiles on neon.

Incident projectile	Process[a]	Cross section (10^{-18} cm^2)		
O^{7+}	SC	29±3	(31.5)[b]	(29)[c]
O^{7+}	SL	0.50±0.06	(0.3)[c]	
C^{6+}	SC	20±2	(22.9)[b]	(17.5±2.5)[d]
C^{6+}	DC	1.90±0.05		
C^{5+}	SC	21±2	(15.7)[b]	
C^{5+}	SL	8.8±0.4		

[a]SC represents single-electron capture, DC represents double-electron capture, and SL represents single-electron loss by the projectile.
[b]These values are taken from Ref. 17 for 1-MeV/u projectiles.
[c]These values are taken from Ref. 18 for 1-MeV/u projectiles.
[d]This value is taken from Ref. 19 for 1.14-MeV/u projectiles.

ion of charge state q_r in coincidence with a cusp electron $\sigma(q_r,e^-)$ and the triple coincidence cross section $\sigma(q_r,q_e,e^-)$ can therefore not be found by fitting the number of coincidences observed with a second-order polynomial in p. The cross sections are therefore extracted from the data in the following way.

(i) The probability per incident projectile ion of producing a recoil ion of charge state q_r, a cusp electron, and, in the case of triple coincidence measurements, a projectile ion of charge state q_e, is calculated from the number of coincidences observed. Errors are statistical.

(ii) The probability that the collision products observed in coincidence are not produced in a single collision but rather in two collisions is found by identifying all paths which lead, via two collisions, to the same final state and then calculating the probabilities associated with those paths. Paths involving three collisions give probabilities which are too small to warrant consideration. The two-collision probabilities can be found as products of the probabilities found in our first set of measurements made at various target-gas pressures. The probabilities found for each of the different paths are summed to yield the total double-collision probability. All errors are differentially propagated.

(iii) The double-collision probabilities found in step (ii) are subtracted from the total probability of producing a given final state found in step (i). The difference yields the probability of reaching this final state in a single collision. Again all errors are differentially propagated.

V. RESULTS AND DISCUSSION

Cross sections for single- and double-electron capture and loss by the projectile extracted from our data are given in Table II and compared with values obtained from a universal empirical scaling rule by Schlacter *et al.*[17] and with single-electron capture and loss cross sections for O^{7+} and single-capture cross sections for C^{6+} measured by Hippler *et al.*[18] and Graham *et al.*[19] The errors in this table and all following tables are relative errors.

Table III gives the cross sections for producing neon recoil ions of charge state q_r in coincidence with projectile ions of charge state q_e assuming an average recoil-ion detection efficiency of 0.014. For C^{6+} projectiles, these cross sections can be compared with those measured by Schuch *et al.*[14] and by Gray, Cocke, and Justiniano.[15] Schuch *et al.*[14] measure the relative cross section for producing a Ne recoil ion of charge state q_r in coincidence with bound-state capture for 10-MeV C^{6+} projectiles on Ne. We find good agreement with their relative values. Our relative values also agree within uncertainties with those of Gray, Cocke, and Justiniano[15] for 1-MeV/u C^{6+} projectiles producing Ne recoil ions in coincidence with

TABLE III. Recoil-ion production cross sections for 1-MeV/u projectiles on neon.

Incident projectile	Process[a]	Cross section (10^{-18} cm^2) $q_r=1+$	$q_r=2+$	$q_r=3+$	$q_r=4+$	$q_r=5+$
O^{7+}	SC	2.0±0.1	7±1	11±2	8±1	3.5±0.2
O^{7+}	NC	345±5	168±2	54±1	13±1	3.5±0.2
O^{7+}	SL	0.07±0.01	0.07±0.04	0.11±0.03	0.13±0.01	0.09±0.02
C^{6+}	SC	2.1±0.4	5.2±0.4	6.5±0.8	4.3±0.4	1.5±0.1
C^{6+}	NC	358±4	204±16	60±6	4.3±0.1	
C^{5+}	SC	2.0±0.4	6.6±0.2	7.6±0.3	4.9±0.1	2.0±0.2
C^{5+}	NC	190±2	84±1	50±1	2.0±0.4	1.0±0.1
C^{5+}	SL	0.53±0.05	2.0±0.4	2.7±0.2	2.2±0.1	0.9±0.1

[a]SC represents single-electron capture, NC represents no charge changing, and SL represents single-electron loss by the projectile.

TABLE IV. Cusp-electron production cross sections for 1-MeV/u projectiles on neon.

Projectile	Cross section (10^{-18} cm^2)
O^{7+}	3.0±0.5
C^{6+}	2.5±0.4
C^{5+}	2.0±0.2

bound-state capture or no charge changing by the projectile. However, the absolute values of our cross sections summed over all recoil-ion charge states are approximately a factor of 2.5 smaller than those of Gray, Cocke, and Justiniano.[15] Our cross sections can be checked for internal consistency by summing the recoil-ion production cross sections in Table III over all recoil-ion charge states for the exit charge states of the projectile $q_e = q_{in} \pm 1$ and thus reproducing the single capture and loss cross sections in Table II to within the experimental error. These cross sections agree well with those measured by other investigators.[17–19] Here we assume that single-electron capture and loss is always associated with the production of a recoil ion. The recoil-ion production cross sections are dominated by the cross section for the production of 1+ recoil ions if the projectile does not change charge. If the projectile captures or loses an electron the production of 2+, 3+, and 4+ recoil ions dominates the cross section. In collisions involving electron loss by O^{7+} projectiles, the highest average recoil-ion charge state is produced. This suggests that the impact parameter required for electron loss by O^{7+} projectiles is smaller than the impact parameter required for target-electron capture by the same projectile, since smaller impact-parameter collisions are expected to produce higher recoil-ion charge states.

Table IV lists the cusp-electron production cross sections. These cross sections cannot be directly compared with previously published cross sections[6] since they depend strongly on how much of the energy and angular distribution of the cusp electrons has been integrated over in the measurement. The detector in our experiment integrates almost over the entire energy and angular distribution of cusp electrons, while previous measurements were made with a half-angle of acceptance of less than 2°. Our measured cusp-electron production cross section for 1-MeV/u C^{6+} projectiles is approximately a factor of 35 larger than that obtained from Ref. 6 by interpolating measured values towards lower energy. Without detailed information about the cusp-electron energy and angular distribution we can only estimate the expected enhancement of our present yield over the yield obtained from Ref. 6. Using a cusp shape as given by Dettmann, Harrison, and Lucas,[20] we estimate approximately an order of magnitude enhancement.

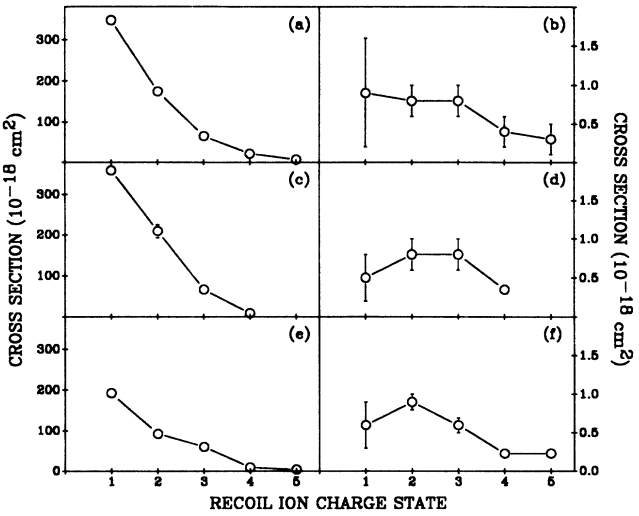

FIG. 3. Cross sections for the production of neon recoil ions of charge state q_r for (a) 1-MeV/u O^{7+}, (c) C^{6+}, and (e) C^{5+} projectiles and cross sections for the cusp-electron production in coincidence with recoil ions of charge state q_r for (b) 1-MeV/u O^{7+}, (d) C^{6+}, and (f) C^{5+} projectiles. Errors are relative errors.

The cross sections for producing a cusp electron in coincidence with a recoil ion of charge state q_r are given in Table V and are compared with the total cross section for producing a recoil ion of charge state q_r in Fig. 3. Figure 3 shows that the probability of producing a 1+ recoil ion is greatly reduced if a cusp electron is also produced in a collision. The recoil-ion charge-state distribution measured in coincidence with a cusp electron is shifted to higher charge states than the recoil-ion distribution measured without the coincidence requirement. The most probable charge states to be found in coincidence with a cusp electron are charge states 2 and 3. The most probable recoil-ion charge state without this coincidence requirement is 1. Summing the cross sections given in Table V for each projectile ion over all recoil-ion charge states we obtain the cusp-electron production cross sections independent of recoil-ion charge states q_r. The values thus obtained agree with the ones given in Table IV to within experimental error.

Table VI lists the triple-coincidence cross sections for the production of a cusp electron, a recoil ion of charge state q_r, and a projectile ion of charge state q_e in a single

TABLE V. Cusp-electron–recoil-ion coincidence cross sections for 1-MeV/u projectiles on neon.

	Cross sections (10^{-18} cm^2)				
Projectile	$q_r=1+$	$q_r=2+$	$q_r=3+$	$q_r=4+$	$q_r=5+$
O^{7+}	0.9±0.7	0.8±0.2	0.8±0.2	0.4±0.2	0.3±0.2
C^{6+}	0.5±0.3	0.8±0.2	0.8±0.2	0.35±0.05	
C^{5+}	0.6±0.3	0.9±0.1	0.6±0.1	0.23±0.04	0.23±0.03

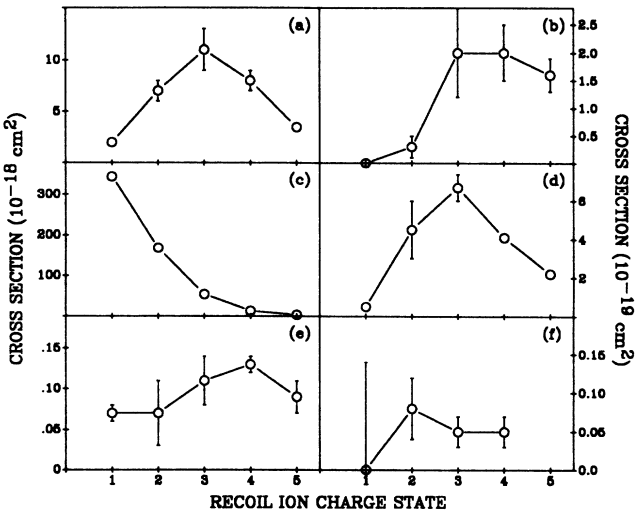

FIG. 4. Cross sections for the production of neon recoil ions by 1-MeV/u O^{7+} projectiles (a) capturing an electron, (c) not changing charge, and (e) losing an electron, and cross sections for recoil-ion–cusp-electron production for projectiles (b) capturing an electron, (d) not changing charge, and (f) losing an electron. Errors are relative errors.

collision. In Fig. 4 we compare these cross sections to those for producing a recoil ion of charge state q_r in coincidence with a projectile ion of charge state q_e without requiring a coincidence with a cusp electron for O^{7+} projectiles. Most cusp electrons accompany a projectile which does not change charge; they are ECC electrons. The recoil-ion charge-state distribution shifts towards higher charge states and closely resembles that measured in coincidence with a bound-state capture without any cusp-electron coincidence requirement. This again points towards a close relationship between bound-state capture and ECC. Target-electron capture by the projectile in coincidence with cusp-electron production shifts the recoil-ion charge-state distribution towards even higher charge states. This process requires at least two target electrons to be involved and therefore happens at smaller impact parameters and leads to higher-recoil-ion charge states. Electron loss by the O^{7+} projectile in conjunction with cusp-electron production causes the recoil-ion

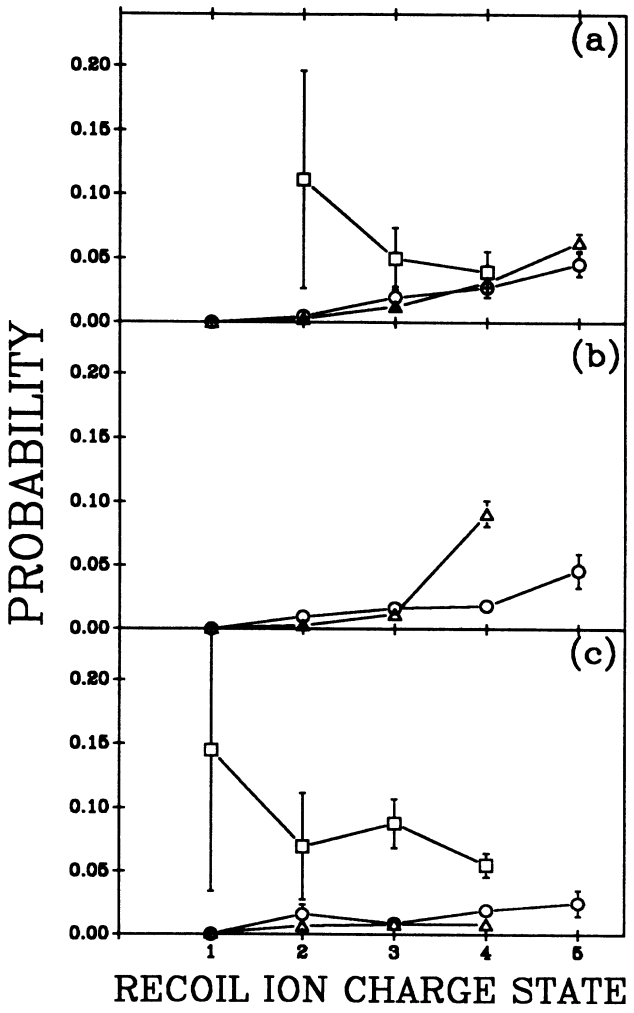

FIG. 5. Probability that, given a recoil ion of charge q_r, a cusp electron is produced in a collision in which the projectile loses an electron (squares), does not change charge (triangles), or captures an electron (circles), for (a) 1-MeV/u O^{7+}, (b) C^{6+}, and (c) C^{5+} projectiles on neon. Errors are relative errors.

charge-state distribution to shift to lower charge states. Thus cusp electrons produced in coincidence with projectile electron loss are often associated with gentler, larger impact-parameter collisions. We can again check our cross sections for internal consistency. By summing the

TABLE VI. Cusp-electron–recoil-ion–projectile-ion coincidence cross sections for 1-MeV/u projectiles on neon.

Projectile[a]		Cross section (10^{-19} cm^2) $q_r=1+$	$q_r=2+$	$q_r=3+$	$q_r=4+$	$q_r=5+$
O^{7+}	SC	0.00	0.3±0.2	2.0±0.8	2.0±0.5	1.6±0.3
O^{7+}	NC	0.5±0.3	4.5±1.5	6.7±0.7	4.1±0.3	2.2±0.2
O^{7+}	SL	0.00+0.14	0.08±0.04	0.05±0.02	0.05±0.02	
C^{6+}	SC	0.00	0.5±0.3	1.1±0.3	0.8±0.2	0.7±0.2
C^{6+}	NC	2.2±1.6	5.9±1.2	7.0±0.7	3.9±0.4	
C^{5+}	SC	0.00	1.0±0.5	0.7±0.3	0.9±0.2	0.5±0.2
C^{5+}	NC	1.8±0.7	5.6±0.7	4.0±0.6	0.16±0.08	
C^{5+}	SL	0.8±0.6	1.4±0.6	2.4±0.5	1.2±0.2	

[a]SC represents single-electron capture, NC represents no charge changing, and SL represents single-electron loss by the projectile.

triple coincidence cross sections over all projectile-ion and all recoil-ion charge states, we reproduce the cusp-electron production cross sections, in Table IV, to within experimental error.

Figure 5 shows the probability that in a collision, from which the projectile emerges with charge q_e and a recoil ion of charge q_r is produced, a cusp electron is also produced. This probability is obtained by dividing the triple-coincidence cross sections in Table VI by the recoil-ion production cross sections in Table III. The probability of producing a cusp electron given the production of a recoil ion increases with increasing recoil-ion charge state for all incident projectile ions that do not change charge or capture a target electron, i.e., the probability of producing an ECC electron increases with increasing recoil-ion charge state. However, the probability of producing a cusp electron given the production of a recoil ion decreases with increasing recoil-ion charge state for C^{5+} and O^{7+} projectiles if it is associated with projectile electron loss. A collision in which a low-charge-state recoil ion is produced and the projectile loses an electron has the highest probability of producing a cusp electron. Overall, the probability of cusp-electron production given the production of a recoil ion is small. We therefore conclude that the production of cusp electrons cannot, by itself, account for the large amount of energy transferred to free electrons in collisions where high recoil-ion charge states are produced.[4,5]

ACKNOWLEDGMENTS

This work was supported in part by the National Science Foundation and by the U.S. Department of Energy, Office of Basic Energy Sciences, Division of Chemical Sciences, under Contract No. DE-AC05-840R21400, with Martin Marietta Energy Systems, Inc.

[1]P. Richard, I. L. Morgan, T. Furuta, and D. Burch, Phys. Rev. Lett. **23**, 1009 (1969).

[2]R. E. Olson, *Electronic and Atom Collisions* (Elsevier, Amsterdam, 1988), p. 271.

[3]C. L. Cocke, Phys. Rev. A **20**, 749 (1979).

[4]R. Schuch, H. Schöne, P. D. Miller, H. F. Krause, P. F. Dittner, S. Datz, and R. E. Olson, Phys. Rev. Lett. **60**, 925 (1988).

[5]H. Schöne, R. Schuch, S. Datz, P. F. Dittner, J. P. Giese, H. F. Krause, M. Schulz, and Q. C. Kessel, Nucl. Instrum. Methods B **40/41**, 141 (1989).

[6]M. Breinig, S. B. Elston, S. Huldt, L. Liljeby, C. R. Vane, S. D. Berry, G. A. Glass, M. Schauer, I. A. Sellin, G. D. Alton, S. Datz, S. Overbury, R. Laubert, and M. Suter, Phys. Rev. A **25**, 3015 (1982).

[7]B. Kraessig, A. D. González, S. Hagmann, and T. B. Quinteros (unpublished).

[8]J. H. McGuire and L. Weaver, Phys. Rev. A **16**, 41 (1977).

[9]R. E. Olson, J. Phys. B **12**, 1843 (1979).

[10]R. E. Olson, J. Ullrich, and H. Schmidt-Böcking, J. Phys. B **20**, L809 (1987).

[11]R. E. Olson, J. Ullrich, and H. Schmidt-Böcking, Phys. Rev. A **39**, 5572 (1989).

[12]W. C. Wiley and I. H. McLaren, Rev. Sci. Instrum. **26**, 1150 (1955).

[13]T. S. Green and G. A. Proca, Rev. Sci. Instrum. **41**, 1409 (1970).

[14]R. Schuch, S. Datz, P. F. Dittner, R. Hippler, H. F. Krause, and P. D. Miller, Nucl. Instrum. Methods **A262**, 6 (1987).

[15]T. J. Gray, C. L. Cocke, and L. Justiniano, Phys. Rev. A **22**, 849 (1980).

[16]R. Hippler, S. Datz, P. D. Miller, P. L. Pepmiller, and P. F. Dittner, Phys. Rev. A **35**, 585 (1987).

[17]A. S. Schlachter, W. G. Graham, K. H. Berkner, R. V. Pyle, A. S. Stearns, and J. A. Tanis, Phys. Rev. A **27**, 3372 (1983).

[18]R. Hippler, S. Datz, P. D. Miller, and P. L. Pepmiller, Z. Phys. D **8**, 163 (1988).

[19]W. G. Graham, K. H. Berkner, R. V. Pyle, A. S. Schlachter, J. W. Stearns, and J. A. Tanis, Phys. Rev. A **30**, 722 (1984).

[20]K. Dettmann, K. G. Harrison, and M. W. Lucas, J. Phys. B **7**, 269 (1974).